SINERGI Vol. 30, No. 3, October 2026: 731-746
http://publikasi.mercubuana.ac.id/index.php/sinergi
http://doi.org/10.22441/sinergi.2026.3.005

Influence of inorganic content on hydrochar quality from high-ash agar extraction waste via hydrothermal carbonization

Andi Firdaus Sudarma[1,2], Edy Hartulistiyoso[1,3]*, Yohanes Aris Purwanto[1], Leopold Oscar Nelwan[1,3], Obie Farobie[1,4], Nono Darsono[5], Khuzaimah Arifin[6], Maharani Dewi Solikhah[1,5], Tri Yulni[1,7], Imam Hidayat[2], Muhamad Fitri[2], and Edy Herianto Majlan[8]
[1]Division of Biosystem Engineering, Faculty of Engineering and Technology, IPB University, Indonesia
[2]Department of Mechanical Engineering, Faculty of Engineering, Universitas Mercu Buana, Indonesia
[3]Center for Research on Engineering Application in Tropical Agriculture (CREATA), IPB University, Indonesia
[4]Surfactant and Bioenergy Research Center (SBRC), IPB University, Indonesia
[5]Research Center for Fuel Technology, National Research and Innovation Agency (BRIN), Indonesia
[6]Research Center for Energy Materials, National Research and Innovation Agency (BRIN), Indonesia
[7]Research Center for Equipment Manufacturing Technology, National Research and Innovation Agency (BRIN), Indonesia
[8]Fuel Cell Institute, Universiti Kebangsaan Malaysia, Malaysia

Abstract
Agar solid waste (ASW) has potential as a feedstock for hydrochar production because of its organic content; however, its high inorganic fraction, predominantly silica, limits its application. Furthermore, studies specifically investigating the hydrothermal carbonization (HTC) of ASW remain limited, given its high ash content and low energy value. This study investigated the HTC of ASW at varying temperatures (180–220 °C) and reaction times (30–90 minutes), with particular emphasis on how two inorganic components (celite versus perlite) affect hydrochar yield, composition, and energy properties. The resulting hydrochars were characterized using CHNSO, proximate, SEM, and FTIR analysis. The results revealed high ash contents reaching 77.7–92.08%, corresponding to HHV of 2.3–3.4 MJ kg^{-1}, while FTIR spectra confirmed strong silica presence through prominent Si–O–Si absorption bands. Therefore, the study provides valuable insights into silica-rich biomass behavior during HTC. The study also evaluated the relationship between HHV and ash content and analyzed the kinetic model. The results demonstrate the significant influence of inorganic components on carbonization pathways, highlighting opportunities to enhance hydrochar quality through pretreatment strategies such as acid/alkaline leaching or mineral separation.

Keywords:
Fuel;
Hydrochar;
Hydrogen;
Hydrothermal Carbonization;
Agar Solid Waste;

Article History:
Received: July 12, 2025
Revised: December 19, 2025
Accepted: June 12, 2026
Published: October 2, 2026

Corresponding Author:
Edy Hartulistiyoso
Department of Mechanical and Biosystem Engineering, IPB University, Indonesia
Email:
edyhartulistiyoso@apps.ipb.ac.id

INTRODUCTION

The annual generation of solid waste from the agar extraction process (ASW) poses a significant environmental concern, particularly in countries with high agar production, such as Indonesia. It is estimated that the agar industry in Indonesia produced 180–550 tons/year of agar in 2020, while the agar yield from seaweed ranges from 17–43% [1][2]. This indicates that a significant portion of the seaweed's organic components remains as waste. This waste is composed mainly of silicates 49.18%, holocellulose 17.7%, alpha-cellulose 14.26%, hemicellulose 1.65%, and lignin 1.12%, a composition that highlights both the scale of the waste problem and the potential for resource recovery through effective waste characterization and valorization [1,3,4]. Improper management of industrial waste has been linked to ecological degradation and public health risks [5,6,7,8,9]. By

applying valorization strategies, the agar industry could reduce its environmental impact while supporting renewable energy and circular economy initiatives.

To address these challenges, hydrothermal carbonization (HTC) is a promising valorization strategy for increasing biomass energy content. Compared to other thermochemical techniques, including gasification and pyrolysis, HTC operates under relatively mild conditions, making it an energy-efficient and environmentally friendly option for processing macroalgae [15].

HTC offers distinct advantages for wet biomass treatment because it avoids energy-intensive drying steps and produces a carbon-rich solid product known as hydrochar [16,17,18]. Consequently, HTC is particularly suitable for treating food waste, municipal solid waste (MSW), and other organic materials, enhancing energy recovery and reducing waste volume [19][20].

Previous studies have demonstrated significant improvements in fuel properties of hydrochar produced from different biomass sources [10,11,12,13,14]. Based on these findings, existing HTC studies can generally be categorized into three groups by feedstock type: terrestrial plant biomass, industrial/municipal waste, and marine algae biomass. Lignocellulosic biomass typically exhibits low ash content (<5%) and produces hydrochar with relatively high HHVs of 24–29 MJ kg^{-1} [21]. Similarly, sewage sludge with moderate ash content (5–15%) can produce hydrochar with HHVs ranging from 23–25 MJ kg^{-1}. In contrast, algae-derived and mineral-rich biomass, characterized by higher ash contents (>20%), generally exhibit lower HHVs (8–21 MJ kg^{-1}) because inorganic components inhibit carbonization [14]. However, ASW, which contains extremely high silica content (>75% ash), falls outside this established range, and its HTC behavior has not yet been systematically evaluated.

To clarify this study's position relative to previous HTC studies on biomass treatment, Table 1 compares ash content and the HHV of the resulting hydrochar. The table shows that ASW exhibits a unique combination of significantly higher ash content and lower HHV than previously studied biomass feedstocks, indicating distinct HTC behavior not addressed in earlier studies of feedstocks with similar characteristics.

Among the reported studies, the anaerobic digestion waste investigated by de Oliveira et al. exhibited ash content values closer to those of ASW. The ash content of the raw sample increased from 38.1% to 64.2% after HTC treatment.

Table 1. HHV and Ash Content of Various Organic Waste and Marine-Based Feedstock Compared to Its Hydrochar Yield

Biomass Source	Raw Feedstock		Hydrochar		Key Observation
	Ash (%)	HHV (MJ/kg)	Ash (%)	HHV (MJ/kg)	
Potato peel [10]	-	-	5.5	9.5	Lower energy content, with low ash content
Sugarcane residues [11]	12.34	19.7	12.0	21.43 – 24.94	High energy densification, with moderate ash content
Anaerobic digestion waste [12]	38.1	13.1	52.8 – 64.2	6.9–13.1	Low HHV. High ash content, and significantly increases after HTC
Sewage sludge [13]	35.3	18.3	61.4 – 66.3	19.3–26.2	High energy content. Ash content significantly increases after HTC
Macroalga *Ulva Lactuca* [14]	11.90	12.04	9.4–23.22	14.96 – 21.22	Mineral-rich. Moderate HHV
ASW (this study)	>75	<5	>75	<5	Silica-dominated. Very high ash content and very low HHV.

In addition, the HHV of the hydrochar produced at 200 °C remained relatively unchanged compared to the raw sample. However, the hydrochar produced at 240 °C showed a 2% reduction in HHV. These findings suggest that the HTC process, particularly at higher temperatures, increases ash concentration, which subsequently lowers HHV [12].

Another key challenge in applying HTC to ASW is its high inorganic content. A significant portion of this inorganic fraction comes from filtration aids used during agar extraction, typically celite (diatomaceous earth) or perlite, both silica-rich minerals [3,4,22]. Silica significantly increases ash content and reduces the combustible fraction of the biomass, thereby lowering the HHV of both raw materials and hydrochar products [23][24]. In

addition, high ash content may cause operational challenges in thermochemical conversion systems [25].

Although several studies have explored the valorization of agar-processing residues, no previous work has specifically investigated HTC treatment of ASW considering different filtration aids (celite versus perlite) nor evaluated their influence on hydrochar properties. Therefore, this study aims to address this gap by systematically analyzing the hydrothermal carbonization of agar solid waste with distinct mineral compositions, with particular emphasis on how inorganic components influence hydrochar yield, composition, and energy properties. The findings are expected to clarify the limitations associated with high-ash biomass and provide insights into improving hydrochar quality, including potential pretreatment strategies for inorganic removal. Furthermore, this study contributes to a broader understanding of the opportunities and challenges in applying HTC to marine-based industrial biomass waste for solid fuel applications.

METHOD

The ASW used in this study was collected from agar extraction plants using *Gracilaria sp.* (GRA) as raw material in Western Java (Plant A) and Eastern Java (Plant B), Indonesia. ASW-A, obtained from Plant A, contains celite (diatomaceous earth), which was added during the filtration stage of the extraction process [26]. In contrast, ASW-B, sourced from Plant B, contains perlite, an amorphous silicate used for the same purpose. Both filtration materials are rich in silica, with celite containing approximately 90% silica and perlite about 75% [27,28,29], contributing significantly to the high inorganic content of the resulting ASW.

Sample Preparation and HTC Treatment

The sample preparation process flow is visually illustrated in Figure 1. Before the HTC experiments, the raw ASW was dried under direct sunlight for approximately 30–40 hours (3-4 days), depending on weather conditions. During this period, ambient temperatures ranged from 30–35 °C, and relative humidity ranged from 60–80%, which may have slightly influenced the drying rate. The dried biomass was then ground, and particles passing through a 40-mesh sieve were collected for further processing.

We conducted HTC experiments using a 100 mL high-temperature and high-pressure stirred batch reactor (BTC-3000, Berghof, Germany), as illustrated in Figure 2. Previous work describes the detailed reactor specifications [30].

For each experiment, 4 g of ASW were mixed with 60 mL of deionized water (1:15 biomass-to-liquid ratio) and loaded into the reactor. The reactor was then sealed, and nitrogen gas was introduced to purge the chamber and establish an inert atmosphere. The mixture was continuously stirred at 900 rpm using an internal magnetic stirrer.

After reaching the target temperature, the internal system was pressurized to 9 MPa and maintained for the desired reaction time.

HTC treatment was carried out at three target temperatures (180 °C, 200 °C, and 220 °C) with a constant heating rate of 2.5 °C/min. Each reaction condition was maintained for 30, 60, or 90 minutes. All HTC characterizations were conducted in triplicate, and the reported values represent the average results with standard deviation (±SD).

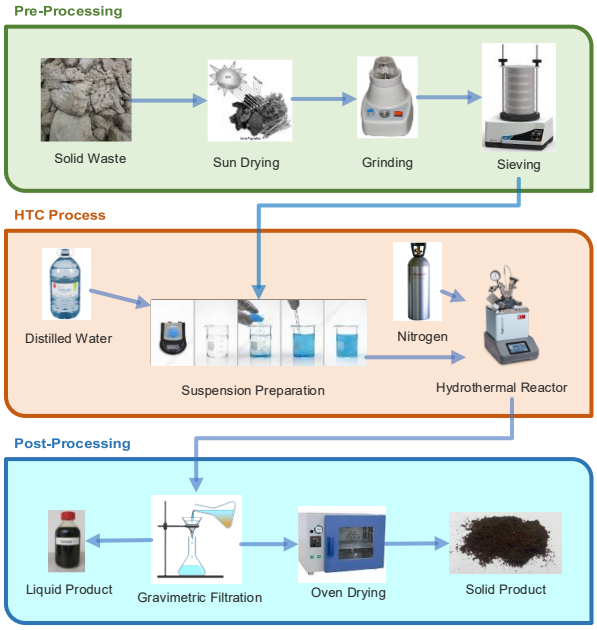

Figure 1. Schematic Representation of The HTC Sample Preparation Process

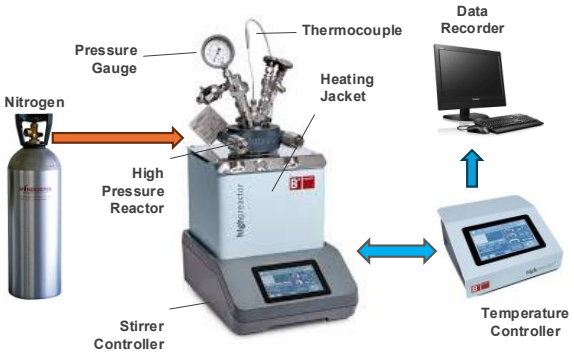

Figure 2. HTC Experimental Setup

After completion of the reaction, the reactor was cooled to below 60 °C before opening. We separated the solid and liquid products by gravimetric filtration. The recovered hydrochar was subsequently dried in an oven at 105 °C for 24 hours to remove residual moisture. Table 2 summarizes the experimental conditions and corresponding sample codes.

Characterization Methods

The hydrochar obtained from the hydrothermal process was examined for ultimate analyses, proximate analysis (ash content), surface morphology, and functional groups. We characterized both samples before and after HTC to assess the process effects, as shown in Figure 3.

The elemental composition of hydrochar was characterized using an elemental (C, H, N, S) analyzer. Meanwhile, Hydrochar was analyzed using Fourier Transform Infrared Spectroscopy (FTIR) over 600–4000 cm^{-1} to evaluate the presence of functional groups. The hydrochar morphology was also examined by scanning electron microscope (SEM).

To comprehensively assess the material, both ultimate and proximate analyses were performed to quantify its elemental composition, including carbon (C), hydrogen (H), nitrogen (N), sulfur (S), and oxygen (O), as well as ash content, fixed carbon (FC), moisture, and volatile matter (VM), all reported in weight percentages. Oxygen content was calculated by difference using the following equation: O (%) = 100% − (%C + %H + %N + %S + %Ash).

Table 2. Hydrothermal Treatment Parameters. ASW-A-0 and ASW-B-0 Refer to Raw Solid Waste Samples Before HTC Treatment

Sample Code	T (°C)	t (min)
ASW-A-0	-	-
ASW-A-1	180	30
ASW-A-2	180	60
ASW-A-3	180	90
ASW-A-4	200	30
ASW-A-5	200	60
ASW-A-6	200	90
ASW-A-7	220	30
ASW-A-8	220	60
ASW-A-9	220	90
ASW-B-0	-	-
ASW-B-1	180	30
ASW-B-2	180	60
ASW-B-3	180	90
ASW-B-4	200	30
ASW-B-5	200	60
ASW-B-6	200	90
ASW-B-7	220	30
ASW-B-8	220	60
ASW-B-9	220	90

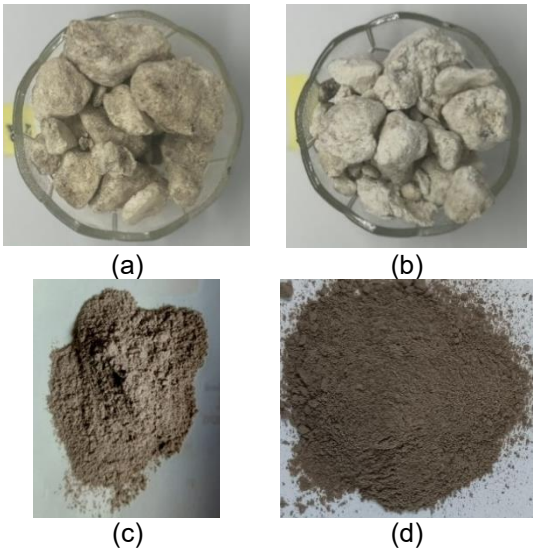

Figure 3. ASW Feedstock and ASW Hydrochar Physical Appearance; (a) ASW-A-0, (b) ASW-B-0, (c) Hydrochar ASW-A, (d) Hydrochar ASW-B

The HHV of the samples was estimated based on a predictive correlation developed by Demirbas et al. [31], as expressed in (1):

$$HHV\left(\frac{MJ}{kg}\right) = 0.316 * C + 1.423 * H + 0.308 * S - 0.154 * O - 0.145 * N \quad (1)$$

In this equation, C, H, N, S, and O denote the respective elemental contents on a dry basis.

RESULTS AND DISCUSSION

This section presents the results of HTC product characterization from ASW. The HTC experiments were conducted at various temperatures and residence times to evaluate how process parameters affect hydrochar production.

The discussion includes hydrochar yield, comprehensive characterization using FTIR and SEM analyses, elemental composition and atomic ratio analysis, proximate analysis, and the HHV of the resulting hydrochar.

Solid Product Fraction

Temperature and time are the most significant parameters influencing liquid, solid, and gas product distribution. As Liu et al. reported, temperature enables the decomposition of macromolecular biomass structures [32].

Figure 4 shows the product yield distribution of hydrochar derived from ASW-A (a) and ASW-B (b) at various residence times and temperatures. It reveals that the solid yield of ASW-B hydrochar remains within a relatively narrow range, approximately 75.4–79.1% (average 77%), across

all experimental conditions. In contrast, ASW-A hydrochar exhibits a wider variation in solid yield, ranging from 67.8–85.8% (average 80.4%). At 220 °C, ASW-A produced lower solid yields, and longer reaction times generally further reduced solid yield.

These results are consistent with findings reported in previous studies, which observed similar reductions in hydrochar yield with increasing temperature and residence time [14]. This behavior is commonly attributed to enhanced deoxygenation reactions, decomposition of organic components, and the formation of water-soluble and volatile compounds during the HTC process.

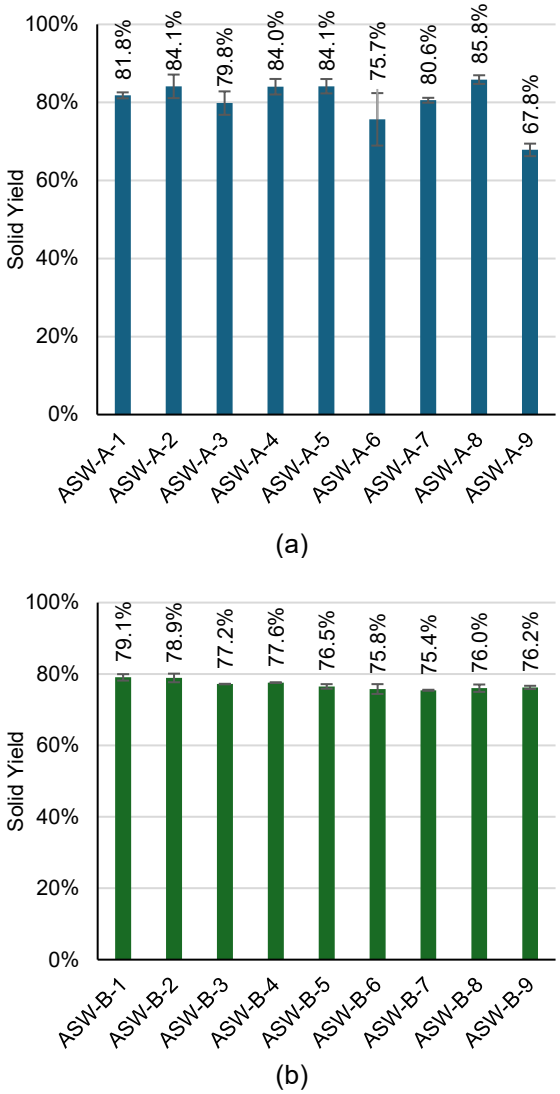

Figure 4. Yield of Hydrochar from ASW at Various Temperatures and Holding Times, (a) ASW-A, (b) ASW-B

The high solid yield from the ASW feedstock indicates a large fraction of thermally stable inorganic materials, particularly silica, which remains in the solid phase regardless of HTC severity. Compared to hydrochar yields derived from pure macroalgae feedstock reported in previous studies (as shown in Table 1), the hydrochar fraction obtained from ASW can reach more than twice the amount. For example, Farobie et al. reported hydrochar yields of 17–32%, while Shrestha et al. reported yields of 9.51- 24.43% [14][33]. The current study's findings are more comparable to those of de Oliveira et al., who investigated sewage sludge with a high ash content of 66%, resulting in hydrochar yields of 59.0–90.2% [12]. These results suggest that high ash content may inhibit the transformation of solid compounds during HTC, thereby retaining a larger fraction of material in the solid phase.

Figure 4(a) shows that ASW-A exhibits a more dynamic fraction distribution. In contrast, ASW-B remains relatively stable, with only approximately ±2% variation across different HTC conditions, as shown in Figure 4(b). This behavior likely reflects the different types of filtration aids present in the ASW samples. Although the ash content of ASW-B is lower, perlite appears to more strongly restrain the decarboxylation process, as indicated by the relatively constant carbon content under varying operational parameters. At the same time, the oxygen content also remains relatively stable with a slight increasing trend, as presented in Table 4.

In contrast, celite in ASW-A tends to be more separable, for example under acidic conditions, than perlite in ASW-B. However, both samples contain high silica content that reacts strongly with hydrofluoric acid (HF), as reported in [34]. Although the ash content of ASW-B is lower, the perlite particles appear to be more strongly bonded to the organic fibers of ASW than the celite particles in ASW-A, as observed in the SEM images presented in Figure 7. The figure shows that the organic content surrounding the celite particles is barely noticeable, whereas in ASW-B, the organic components appear to overlap Interact more closely with the perlite particles, which may influence the HTC reaction process.

Proximate Analysis of Hydrochar

Table 3 shows the proximate analyses of ASW feedstock and ASW hydrochar produced through HTC. One notable characteristic of ASW is its exceptionally high ash content, which fundamentally distinguishes it from typical lignocellulosic biomass and limits its suitability as a solid fuel feedstock.

Table 3. Proximate (Moisture, Volatile Matter, Ash, Fixed Carbon) Compositions of ASW and Hydrochar, Reported in wt.%. N/D Indicates "Not Detected," and N/A Indicates "Not Available"

Feedstock	Moisture	VM	Ash	FC
ASW-A-0	3.78 ± 0.02	11.09 ± 0.03	85.12 ± 0.04	0.015 ± 0.001
ASW-A-1	1.82 ± 0.04	6.96 ± 0.02	91.45 ± 0.03	N/D
ASW-A-2	1.79 ± 0.04	7.57 ± 0.04	90.96 ± 0.03	N/D
ASW-A-3	1.76 ± 0.03	8.40 ± 0.04	90.08 ± 0.01	N/D
ASW-A-4	1.87 ± 0.05	6.63 ± 0.03	91.76 ± 0.05	N/D
ASW-A-5	1.52 ± 0.03	6.79 ± 0.06	91.86 ± 0.07	N/D
ASW-A-6	1.61 ± 0.02	6.80 ± 0.06	91.73 ± 0.03	N/D
ASW-A-7	1.65 ± 0.01	7.91 ± 0.01	90.74 ± 0.06	N/D
ASW-A-8	1.57 ± 0.01	6.74 ± 0.04	91.90 ± 0.06	N/D
ASW-A-9	1.41 ± 0.02	6.73 ± 0.07	92.08 ± 0.02	N/D
ASW-B-0	4.89 ± 0.03	27.78 ± 0.04	77.10 ± 0.02	3.46 ± 0.02
ASW-B-1	N/A	N/A	76.10 ± 0.07	N/A
ASW-B-3	N/A	N/A	77.33 ± 0.04	N/A
ASW-B-4	N/A	N/A	76.77 ± 0.04	N/A
ASW-B-6	N/A	N/A	75.42 ± 0.01	N/A
ASW-B-7	N/A	N/A	77.30 ± 0.05	N/A
ASW-B-9	N/A	N/A	77.70 ± 0.05	N/A

Table 4. Elemental (C, H, N, S, O) Compositions of ASW and Hydrochar, Reported in wt%. N/D Indicates "Not Detected"

Feedstock	C	H	N	S	O	HHV (MJ/kg)
ASW-A-0	4.69 ± 0.05	1.26 ± 0.02	N/D	0.028 ± 0.001	8.90 ± 0.03	1.91 ± 0.03
ASW-A-1	1.97 ± 0.08	0.82 ± 0.01	N/D	0.041 ± 0.002	5.72 ± 0.06	0.92 ± 0.02
ASW-A-2	2.05 ± 0.04	0.81 ± 0.01	N/D	0.041 ± 0.002	6.14 ± 0.05	0.87 ± 0.02
ASW-A-3	2.03 ± 0.05	0.81 ± 0.01	N/D	0.042 ± 0.002	7.04 ± 0.04	0.72 ± 0.02
ASW-A-4	1.67 ± 0.06	0.78 ± 0.02	N/D	0.041 ± 0.003	5.75 ± 0.04	0.77 ± 0.03
ASW-A-5	1.99 ± 0.05	0.79 ± 0.02	N/D	0.041 ± 0.003	5.32 ± 0.04	0.95 ± 0.02
ASW-A-6	2.75 ± 0.06	1.00 ± 0.04	N/D	0.042 ± 0.002	4.48 ± 0.01	1.61 ± 0.02
ASW-A-7	3.81 ± 0.08	1.20 ± 0.02	N/D	0.041 ± 0.001	4.21 ± 0.04	2.28 ± 0.04
ASW-A-8	1.79 ± 0.04	0.85 ± 0.02	N/D	0.041 ± 0.002	5.42 ± 0.02	0.95 ± 0.02
ASW-A-9	1.85 ± 0.06	0.91 ± 0.01	N/D	0.058 ± 0.003	5.10 ± 0.05	1.11 ± 0.03
ASW-B-0	9.83 ± 0.07	1.70 ± 0.01	0.29 ± 0.01	N/D	11.09 ± 0.05	4.80 ± 0.04
ASW-B-1	9.78 ± 0.04	1.57 ± 0.01	0.38 ± 0.02	N/D	12.17 ± 0.04	3.40 ± 0.02
ASW-B-3	9.13 ± 0.04	1.49 ± 0.01	0.17 ± 0.02	N/D	11.87 ± 0.01	3.16 ± 0.03
ASW-B-4	9.05 ± 0.06	1.48 ± 0.01	0.25 ± 0.01	N/D	12.44 ± 0.01	3.02 ± 0.02
ASW-B-6	9.46 ± 0.06	1.51 ± 0.01	0.13 ± 0.02	N/D	13.48 ± 0.02	3.05 ± 0.03
ASW-B-7	9.23 ± 0.02	1.47 ± 0.01	0.29 ± 0.01	N/D	11.70 ± 0.06	3.17 ± 0.02
ASW-B-9	8.51 ± 0.05	1.40 ± 0.01	0.35 ± 0.03	N/D	12.04 ± 0.04	2.78 ± 0.02

The ash fraction of untreated ASW reaches 77–86 wt.%, compared to raw *Gracilaria sp.* biomass that generally contains only 35.04-44.33 wt.% ash [35]. This substantial discrepancy indicates that the mineral content in ASW is not an inherent characteristic of the seaweed itself, but originates predominantly from external mineral additives introduced during agar extraction, particularly celite and perlite. Consequently, the HTC behavior of ASW cannot be interpreted using the conventional framework commonly applied to low-ash biomass, because inorganic dominance strongly governs the thermochemical conversion rather than organic carbon transformation.

In ASW-B, ash content increased slightly from 77.1 wt.% (ASW-B-0) to approximately 77.7% after HTC, while ASW-A showed a more pronounced increase from 85.12–92.08 wt.%. This increase results from the preferential degradation and solubilization of organic fractions through hydrolysis, dehydration, and decarboxylation, while inorganic components remain relatively inert and are retained in the hydrochar matrix [36]. Consequently, the relative mineral concentration increases as volatile and oxygenated organic compounds are removed. These findings are consistent with de Oliveira et al., who reported an increase in ash content from 38.1% to 64.2% after HTC of high-ash sewage sludge, accompanied by a decrease in HHV [12].

The stronger ash enrichment observed in ASW-A further suggests that the type of filtration aid plays a critical role in governing HTC behavior. Celite-based residues appear to promote more pronounced hydrothermal transformation effects than perlite-based residues, likely because the organic fraction in ASW-A is more exposed and accessible to hydrothermal reactions. As a result, organic matter degrades more extensively during HTC, leading to greater loss of volatile and carbonaceous components while the inorganic mineral fraction remains in the solid phase. This selective decomposition consequently intensifies ash enrichment in ASW-A compared with ASW-B.

The reduction in volatile matter (VM) from 11.1 wt.% in raw ASW-A to 6.6–8.4 wt.% after HTC further supports this interpretation. The disproportionate removal of volatile organic compounds relative to inorganic species indicates that HTC selectively decomposed the combustible fraction while leaving most minerals unaffected [37]. Consequently, the process reduced the reactive organic portion without significantly decreasing the inorganic load, which is counterproductive for fuel upgrading. Similar behavior has been reported for other silica-rich biomass such as rice husk, where HTC often increases ash concentration due to mineral enrichment effects rather than improving fuel quality [38].

Despite the unfavorable ash characteristics, HTC treatment improved the hydrophobic behavior of ASW-derived hydrochar, as reflected by the substantial reduction in moisture content. HTC treatment reduced the moisture content of raw ASW-A to as low as 1.52 wt.%. This behavior indicates that HTC enhanced the material's physicochemical stability through progressive dehydration reactions. Under elevated hydrothermal conditions, hydroxyl groups and bound water associated with the biomass structure are removed, reducing hydrophilic functional groups and thereby lowering the hydrochar's affinity for moisture reabsorption. From a fuel-handling perspective, this improvement matters because lower moisture content can enhance storage stability, reduce biological degradation, and improve ignition behavior. Moreover, the resulting moisture content satisfies the requirement of SNI 4931:2010 for coal briquettes, which specifies a maximum moisture content of 12 wt.%. Despite this improvement, the benefit remains insufficient to compensate for the extremely high ash fraction, which continues to dominate the overall fuel characteristics of the hydrochar.

These results show a critical limitation in directly applying HTC to highly mineralized industrial biomass residues. Although HTC is commonly promoted as a carbon densification process, its effectiveness becomes questionable when the feedstock contains excessive inorganic matter. In ASW, the process failed to substantially improve fuel characteristics because dominant silica-rich minerals diluted the combustible carbon fraction and suppressed energy densification. This limitation becomes more evident when compared with the Indonesian fuel briquette standard (SNI 4931:2010), which specifies maximum ash contents of 15 wt.% for class A and 20 wt.% for class B carbonized briquettes. The hydrochars produced in this study remain far beyond these limits, indicating that direct HTC treatment alone is insufficient to produce fuel-grade hydrochar from ASW. Therefore, pretreatment strategies aimed at mineral removal, such as acid leaching, flotation, or selective deashing processes, are not optional process enhancements but essential requirements if ASW-derived hydrochar is to be considered feasible for energy applications.

Ultimate Analysis of Hydrochar

Elemental composition results are presented in Table 4. For ASW-A samples, carbon content ranged from 1.7–3.8 wt.%, indicating that HTC did not substantially enrich the hydrochar's carbon fraction. The hydrogen content decreased from 1.26 wt.% in untreated ASW-A (ASW-A-0) to approximately 0.78 wt.% after HTC, reflecting dehydration reactions during hydrothermal treatment. Similarly, oxygen content ranged from 5.10–8.90 wt.%, suggesting partial removal of oxygen-containing functional groups through dehydration and decarboxylation.

A similar trend was observed for ASW-B samples. The carbon content remained within the range of 8.5–9.8 wt.%, which is higher than that of ASW-A but still substantially lower than values commonly reported for lignocellulosic hydrochar. The comparatively higher carbon retention in ASW-B suggests that perlite-containing residues may impose a less severe dilution effect than celite-rich residues. Moreover, hydrogen content decreased slightly from 1.698% in raw ASW-B to 1.399% after HTC, again confirming dehydration reactions. Meanwhile, oxygen content remained relatively high (11.0–13.48 wt.%), indicating that a considerable portion of oxygenated structures persisted after treatment.

The limited improvement in elemental composition is directly reflected in the calorific performance of the hydrochars. The HHV values ranged from 0.7–3.4 MJ kg^{-1}, substantially lower than those typically reported for biomass-derived hydrochars (see Table 1). Even the highest HHV obtained for ASW-A hydrochar, 2.276 MJ kg^{-1}

(ASW-A-7), remains far below the energy content generally required for practical solid fuel applications. These results are consistent with the findings reported by de Oliveira et al., where the ash content of the raw sample increased after HTC treatment, while the HHV of hydrochar produced at 200 °C remained relatively unchanged compared to the raw sample. Furthermore, hydrochar produced at 240 °C exhibited a 2% reduction in HHV [12]. These findings suggest that the HTC process, particularly at higher temperatures, increases ash concentration, which subsequently lowers HHV. This occurs because a portion of the organic compounds in the feedstock were converted into liquid products during HTC, while another fraction is directly transformed into gaseous products. Simultaneously, liquid intermediates undergo further secondary reactions that generate additional gaseous compounds. As a result, the relative ash concentration in the solid phase increases. These results indicate that HTC alone was ineffective in achieving significant energy densification of ASW. The low HHV values are primarily attributed to the exceptionally high ash fraction and the limited fixed carbon content retained in the hydrochar.

This phenomenon shows that HTC effectiveness depends strongly on feedstock composition. In conventional lignocellulosic biomass, HTC often enhances fuel quality by increasing fixed carbon and reducing oxygenated compounds. However, in highly mineralized feedstocks such as ASW, the process instead promotes mineral enrichment without substantial carbon enhancement. Consequently, the thermochemical conversion pathway shifts from carbon densification toward inorganic concentration. This interpretation is consistent with previous studies on other high-ash biomass systems. De Oliveira et al. reported that anaerobic digestion residues exhibited ash content increases from 38.1–64.2% after HTC, while the HHV remained unchanged or even decreased at higher HTC temperatures [12]. Such behavior indicates that increasing process severity may intensify mineral concentration effects rather than improve fuel quality.

Liu et al. reported similar observations, finding that hydrochar derived from high-ash microalgae exhibited HHVs of only 8.83–9.88 MJ kg^{-1}, significantly lower than hydrochars produced from carbon-rich lignocellulosic biomass [39]. Although the HHVs reported by Liu et al. were still higher than those obtained in the present study, the overall trend confirms that excessive inorganic content strongly limits the carbonization efficiency of HTC. Therefore, the poor energy performance observed in ASW-derived hydrochar should not be interpreted simply as a consequence of "low carbon content," but as evidence that mineral-rich industrial residues fundamentally alter the thermochemical transformation mechanisms during HTC.

Further analysis using the Van Krevelen diagram evaluated the evolution of the atomic hydrogen-to-carbon (H/C) and oxygen-to-carbon (O/C) ratios of raw ASW and the corresponding hydrochars produced through HTC, as shown in Figure 5.

The diagram compares the H/C and O/C ratios; lower values indicate greater material maturity and a stronger resemblance to high-rank coal, which is desirable for fuel applications. In general, all ASW and hydrochar samples remain clustered in the upper-right region of the diagram, characterized by relatively high H/C ratios (>1.5) and O/C ratios ranging from approximately 0.8 to above 1.2. Such positioning indicates that the materials still contain a substantial fraction of oxygenated and hydrogenated functional groups, reflecting the incomplete carbonization of the biomass during HTC. This behavior differs significantly from the typical evolution pathway of lignocellulosic biomass, where HTC commonly induces progressive dehydration and decarboxylation reactions that shift the material toward the lower-left region of the diagram, corresponding to increased aromaticity and carbon enrichment [40].

The ASW-A hydrochars exhibited particularly anomalous behavior. The H/C ratios increased substantially to 3.78–5.90, exceeding the raw ASW-A ratio of approximately 3.2, while the O/C ratios ranged from 0.83–2.6 compared with the raw O/C ratio of 1.4.

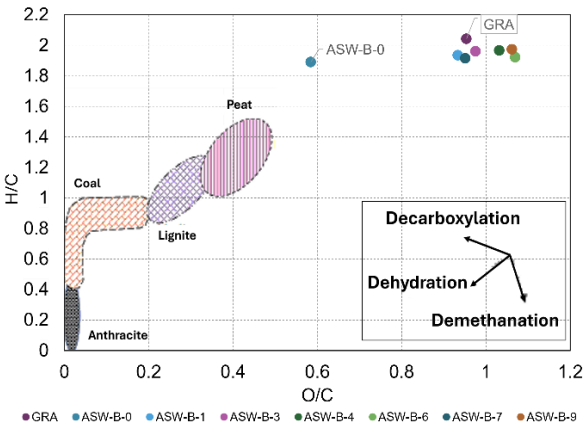

Figure 5. Van Krevelen Diagram of *Gracilaria sp.*, Untreated ASW and ASW Hydrochar from Factory B

These unusually high atomic ratios were not included in Figure 5 because they were positioned far outside the typical region occupied by conventional solid fuels, making direct comparison difficult. Rather than indicating improved fuel quality, these elevated ratios suggest that HTC did not effectively promote carbon condensation in ASW-A. Instead, the process appears to have preferentially removed a limited portion of carbon while retaining oxygenated and hydrogen-containing structures.

The behavior of ASW-B hydrochars was comparatively more stable. The H/C ratios ranged from 1.90–1.97, remaining close to the raw ASW-B ratio of 1.89, while the O/C ratios increased from 0.59 in the raw material to 0.86–1.07 after HTC. Although the changes were less extreme than those observed in ASW-A, the increase in O/C ratio still indicates that HTC did not significantly reduce oxygenated functional groups in the biomass matrix. In conventional HTC systems, decreasing O/C ratios are generally interpreted as evidence of successful dehydration and decarboxylation reactions that improve carbonization. However, the opposite trend observed in ASW-B suggests that oxygen removal was limited.

FTIR Analysis

Figure 6 presents the FTIR spectra of *Gracilaria sp.*, untreated agar solid waste (ASW-A and ASW-B), and selected hydrochar samples (ASW-B-3, ASW-B-6, and ASW-B-9). The FTIR analysis highlights the dominant influence of inorganic constituents on the resulting hydrochar structure. Although the major functional groups remained generally consistent across the samples, absorption intensity varied as HTC severity increased, indicating partial modification of the organic matrix during hydrothermal treatment.

Table 5 summarizes the characteristic band assignments for the raw materials and hydrochars. The broad absorption band centered around 3355 cm^{-1} is associated with O–H stretching vibrations originating from hydroxyl groups in cellulose, polysaccharides, and agarose structures. Meanwhile, the band near 1618 cm^{-1} corresponds to O–H bending vibrations and/or C=O stretching associated with adsorbed water and oxygen-containing functional groups in polysaccharides [45]. These bands are clearly visible in both *Gracilaria sp.* and ASW samples, confirming residual polysaccharide-based organic structures even after agar extraction.

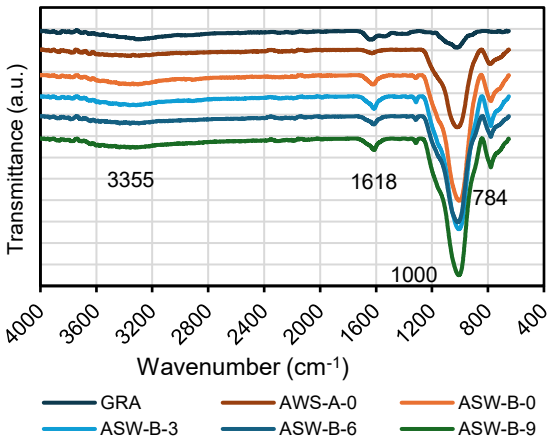

Figure 6. FTIR Spectra of *Gracilaria sp*., Agar Solid Waste and ASW Hydrochar

Table 5. FTIR Band Assignments and Main Peak (cm^{-1}) of *Gracilaria sp.* (GRA), Raw ASW, and ASW Hydrochar Sample. Band Assignment Based on References [1] and [14]

Typical band Assignment	GRA	ASW-A	ASW-B
Si–O–Si bridge bending vibration of oxygen atoms	-	775	780
D-galactose-4-sulfate vibration	-	841	842
Asymmetric stretching of silicate framework (Si–O–Si)	-	1000	1000
Asymmetric O=S=O stretching associated with sulfate groups	-	-	1313
Aromatic C=C stretching vibration	1446	-	-
O–H bending vibration (δOH) of coordinated water molecules	1618	1623	1618
Stretching vibration of hydrogen-bonded hydroxyl (-OH) groups	3355	3399	3331

However, compared with conventional lignocellulosic biomass hydrochar, the FTIR spectra of ASW-derived hydrochar are dominated by inorganic silicate-related bands rather than carbonaceous functional groups. One prominent feature is the strong absorption peak around 1000 cm^{-1}, attributed to asymmetric stretching vibrations of Si–O–Si bonds. In addition, the persistent peak near 780–784 cm^{-1} corresponds to the bending vibration of Si–O–Si bridges [41].

The strong intensity after HTC indicates that silica-rich minerals originating from filtration aids such as celite and perlite remained structurally stable throughout the hydrothermal process. Importantly, these silicate bands are absent in the raw *Gracilaria sp.* spectrum, confirming that the inorganic silica phases are introduced during industrial agar processing.

The dominance of Si–O–Si absorption bands provide strong spectroscopic evidence supporting the ash and elemental analysis results discussed previously. In contrast to typical biomass-derived hydrochar, where aromatic C=C structures often become more pronounced after HTC, the spectra of ASW-derived hydrochar showed relatively weak development of carbonaceous functional groups. For example, the aromatic C=C stretching band observed in raw *Gracilaria sp.* near 1446 cm^{-1} became less distinguishable in the ASW samples, suggesting that the carbonaceous fraction was either relatively low or masked by the dominant inorganic matrix.

Additional evidence of residual sulfur-containing compounds is observed from the absorption band near 1313 cm^{-1} in ASW-B, corresponding to asymmetric O=S=O stretching vibrations associated with sulfate groups. The presence of sulfate-related functional groups is consistent with the chemical composition of agar-derived polysaccharides such as sulfated galactans. Furthermore, the band around 841–842 cm^{-1} assigned to D-galactose-4-sulfate confirms that portions of the original agar-related polysaccharide structure were still retained after processing and HTC treatment.

SEM Analysis

Figure 7 presents the SEM micrographs of ASW-A and ASW-B at 5,000× magnification. The micrographs reveal clear morphological differences between the two residues, primarily associated with the type of filtration aid used during agar extraction. ASW-A is dominated by celite particles embedded within a limited organic matrix, whereas ASW-B exhibits perlite particles more closely associated with residual organic structures. These observations provide additional evidence that the physicochemical behavior of ASW during HTC is strongly influenced by process-derived mineral additives rather than by the intrinsic biomass structure alone.

The inorganic particles in both samples exhibit relatively smooth, rigid surfaces, whereas the organic fraction appears more irregular and heterogeneous.

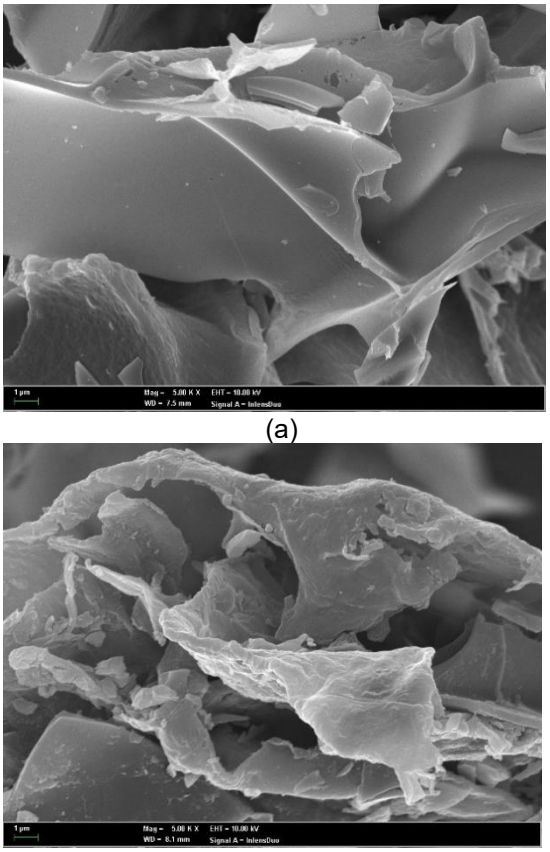

Figure 7. SEM Images at 5,000X; (a) ASW-A, (b) ASW-B

In ASW-A, the celite particles are visually dominant, and the surrounding organic substrate appears minimal or poorly attached to the mineral surface.

In contrast, ASW-B exhibits a more heterogeneous morphology composed of aggregated mineral-organic clusters. The perlite particles appear partially covered or interconnected with residual organic matter, indicating stronger physical interaction between the inorganic and organic phases.

Figure 8 further illustrates the morphological evolution from raw *Gracilaria sp.* to hydrothermally treated ASW samples. The raw *Gracilaria* biomass (Figure 8(a)) exhibits a highly porous and fibrous structure with abundant open channels, characteristic of cellulose- and polysaccharide-rich biomass. This morphology favors mass transfer and hydrothermal reactivity. However, this native structure is largely destroyed during agar extraction, as shown in ASW-B-0 (Figure 8(b)), where the surface becomes compacted, collapsed, and significantly less fibrous.

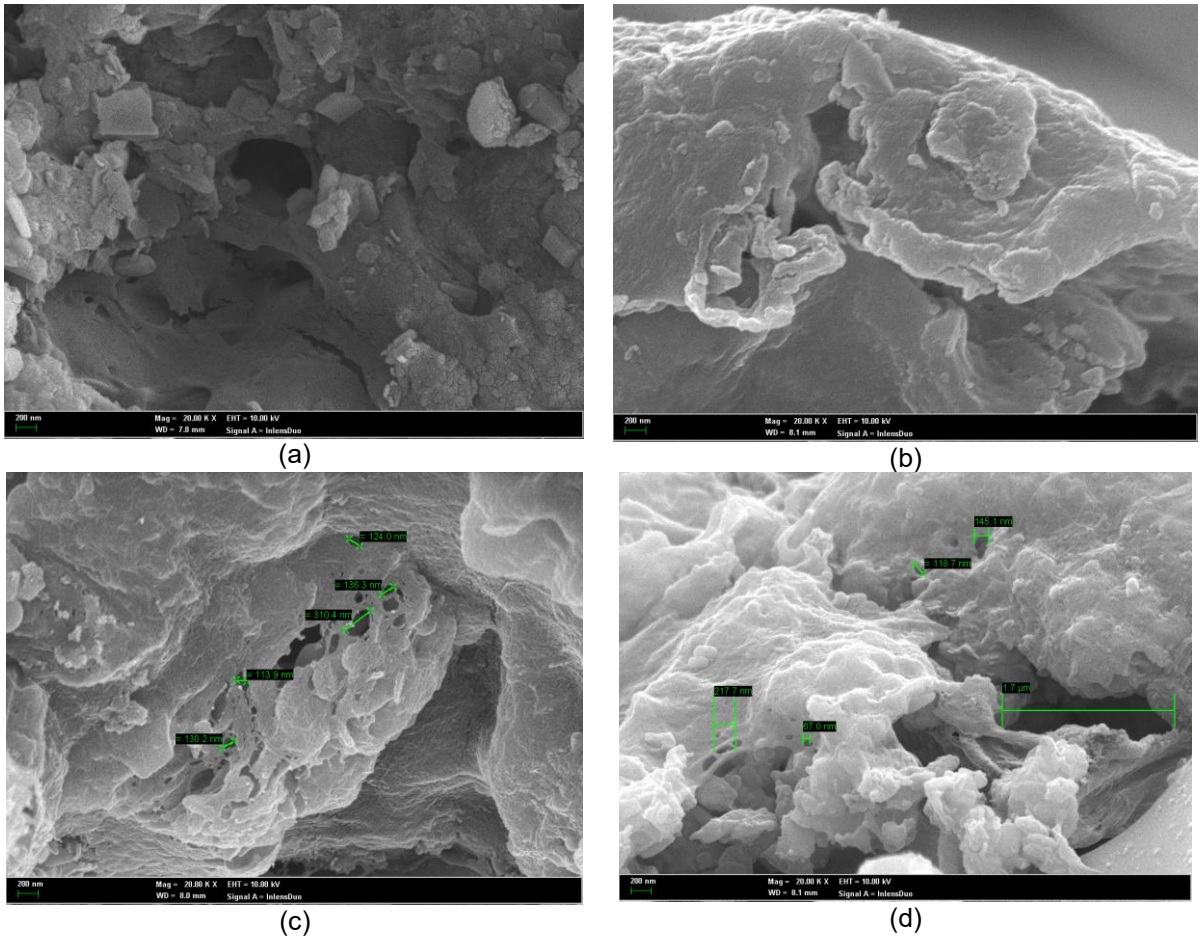

Figure 8. SEM Images of Organic Fibers at 20,000× magnification. (a) GRA, (b) ASW-B-0, (c) ASW-B-6, (d) ASW-B-9

After HTC treatment, additional structural changes become apparent. ASW-B-6 (Figure 8(c)) exhibits a semi-fractured surface with the formation of small internal pores, indicating partial decomposition of residual organic matter during hydrothermal treatment. Meanwhile, ASW-B-9 (Figure 8(d)) shows more pronounced fragmentation and enlarged pores, reflecting progressive degradation of the remaining organic matrix at longer residence times.

Kinetic Model of Ash Content

A kinetic model was developed to evaluate the apparent ash enrichment behavior of ASW-A during HTC and to examine how temperature influences the evolution of ash content.. Unlike conventional HTC studies that focus primarily on carbonization kinetics or hydrochar yield, this work emphasizes ash evolution because mineral accumulation was identified as the dominant phenomenon governing the physicochemical behavior of ASW-derived hydrochar. This approach is particularly important because the unusually high ash content fundamentally altered the feedstock's thermochemical conversion pathway. The kinetic behavior of ash enrichment was described using a first-order reaction model, expressed by (1):

$$\frac{dX}{dt} = k(1 - X) \quad (1)$$

where X represents the ash content as the reaction response, k is the apparent reaction rate constant (s^{-1}), and t is the residence time (s). Although ash itself is not chemically "formed" during HTC, the increase in ash fraction reflects the progressive decomposition and removal of organic matter. At the same time, inorganic minerals remain largely retained in the solid phase. Therefore, the kinetic model can be interpreted as an apparent enrichment process driven by selective degradation of the combustible fraction.

The temperature dependence of the reaction rate constant was evaluated using the Arrhenius equation:

$$k = A \exp\left(-\frac{E}{RT}\right) \quad (2)$$

where A is the pre-exponential factor, E is the activation energy, R is the universal gas constant, and T is the absolute temperature (K).

The rate constants at different temperatures were obtained from the slopes of the linear plots of ( )- ln (1-X) versus residence time. At the same time, the activation energy and pre-exponential factor were estimated from the Arrhenius relationship between $\ln k$ and $1/\mathrm{T}$, as presented in Figure 9(a).

The resulting kinetic expression was determined as:

$$k = 0.1719 \exp\left(-\frac{12148}{8.314T}\right) \quad (3)$$

The calculated activation energy was relatively low (12.15 kJ mol^{-1}) compared with activation energies commonly reported for biomass carbonization or devolatilization reactions [42][43].

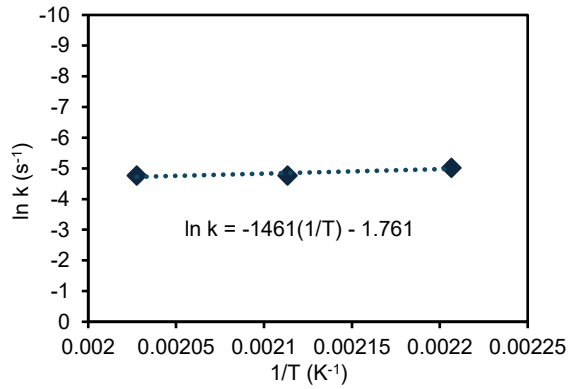

(a)

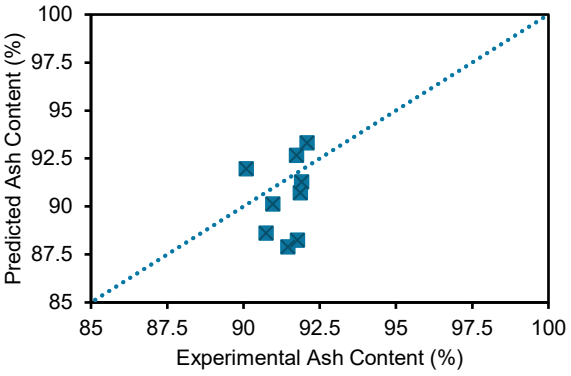

(b)

Figure 9. (a) Arrhenius Plot, and (b) Ash Content from Experiment and Kinetic Model Parity Plot

This comparatively low value suggests that the process was dominated by relatively mild decomposition of organic constituents accompanied by retention and concentration of inorganic minerals.

Figure 9(b) compares the predicted ash content obtained from the kinetic model with the experimental data. The prediction error (0.7–3.8%) indicates that the first-order model adequately describes the apparent ash enrichment behavior during HTC.

Ash Content–HHV Correlation and Future Improvement Strategies for Hydrochar

To further evaluate the influence of mineral content on hydrochar fuel quality, Figure 10 compares the relationship between ash content and HHV obtained in the present study with hydrochars reported in previous studies, including sorghum [44], swine manure [45], *Ulva lactuca* macroalga [14], and industrial digestate (IDT) waste [12]. The comparison reveals a clear inverse relationship between ash content and HHV, confirming that mineral accumulation plays a dominant role in reducing hydrochar energy performance.

Feedstocks with low ash content generally produced hydrochars with substantially higher calorific values. Sorghum-derived hydrochar, for example, exhibited ash contents of only 3.5–4.3 wt% and achieved HHVs of 20.2–25.2 MJ kg^{-1}. In contrast, ASW-A hydrochars contained extremely high ash contents of approximately 90–92.8 wt%, corresponding to very low HHV (0.7–2.3 MJ kg^{-1}). This comparison shows that ash content is not merely a secondary compositional parameter, but a critical factor governing thermochemical upgrading efficiency during HTC.

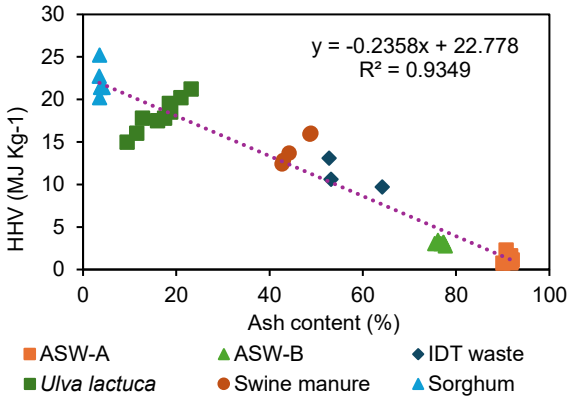

Figure 10. Relation of ash content to HHV of HTC products, comparison of hydrochar ASW from current work with other hydrochar from various feedstocks.

The strong relationship between ash content and HHV also suggests that ash concentration may serve as an important indicator for evaluating and controlling HTC performance.

The results imply that optimizing HTC parameters alone may be insufficient for highly mineralized feedstocks such as ASW, because the dominant limiting factor stems from feedstock composition rather than solely from reaction severity. Figure 6 further shows that ash content correlates strongly with HHV, with the fitted relationship exhibiting high coefficients of determination ($R^2 > 0.9$).

Despite the unfavorable fuel properties, HTC initiated thermochemical transformations within the organic fraction, as indicated by changes in elemental composition, reduced moisture, and volatile matter. Although carbon enrichment was limited, these changes confirm that the organic matrix remained reactive under hydrothermal conditions. Thus, poor hydrochar quality results not from the absence of conversion, but from the dominant influence of retained mineral constituents that mask improvements in the carbonaceous phase. ASW HTC should therefore be viewed as a constrained carbonization system in which organic transformation occurs, but inorganic retention dominates.

The distinctive HTC behavior of ASW creates opportunities beyond conventional fuel applications. Rather than being viewed solely as a disadvantage, its high ash content may enhance the functional potential of mineral-enriched hydrochar. The combination of silica-rich minerals and residual carbon structures could support applications as sorbents, catalyst supports, or silica-based functional materials after appropriate modification. Roberts et al. reported promising biosorption performance of ASW-derived biochar due to its porous structure and surface functionality [26], suggesting greater potential for environmental remediation than direct solid-fuel use.

Nevertheless, if energy applications remain the primary target, substantial mineral reduction is essential. Previous work conducted by our research group demonstrated that hydrofluoric acid (HF) leaching significantly reduced the ash content of ASW from 85.8 wt% to 43.2 wt%, accompanied by an increase in HHV from 1.9 to 6.1 MJ kg^{-1} [34]. Although the resulting fuel quality remained below that of conventional biomass hydrochar, the improvement clearly confirms that silica removal can substantially enhance the energetic properties of ASW-derived materials. Similar trends have been reported in other high-ash biomass systems. Ekanthalu et al. investigated acid-assisted HTC of sewage sludge and reported that reducing the ash fraction significantly improved hydrochar HHV to 14.1 MJ kg^{-1} [46]. This finding further supports the conclusion that the low calorific value observed in untreated hydrochar is fundamentally linked to mineral dilution effects rather than to the inability of the organic fraction to undergo thermochemical conversion.

Beyond hydrochar production, ASW also presents opportunities for integrated resource recovery. Li et al. reported that valuable products such as bioactive oligosaccharides and reusable perlite can be recovered from agar industry waste streams [22]. Their findings indicate that the recovered perlite retained suitable physicochemical properties for industrial reuse, showing that agar waste should not be regarded merely as a low-quality fuel precursor but as a multi-component industrial residue with potential for circular resource utilization.

Future research should integrate pretreatment strategies with HTC to overcome excessive mineral content. Silica removal before HTC may improve carbonization efficiency, while post-treatment upgrading could further enhance fuel quality. Reducing inorganic compounds is expected to increase energy content; for example, Shin et al. reported that inorganic metal- and acid-derived catalysts increased hydrochar calorific value by 18% compared with coal for power generation [47].

Future studies should also quantify the liquid and gaseous products generated during HTC, as the present study focused mainly on the solid hydrochar fraction. A comprehensive mass and energy balance across all phases would provide deeper insight into conversion pathways, resource-recovery potential, and the overall feasibility of ASW hydrothermal processing.

CONCLUSION

Hydrothermal carbonization (HTC) of agar extraction solid waste (ASW) was investigated using celite-based ASW-A and perlite-based ASW-B at 180–220 °C for 30–90 min. Unlike conventional lignocellulosic biomass, ASW conversion was governed primarily by inorganic mineral phases rather than carbon densification. FTIR, ash, elemental, SEM, and Van Krevelen analyses confirmed that silica-rich minerals remained structurally stable and accumulated in the hydrochar matrix. Consequently, the hydrochars exhibited very low HHVs (0.7–3.4 MJ kg^{-1}), despite dehydration and partial transformation of the organic fraction. ASW-B showed relatively stable solid yields (75.4–79.1 wt%), whereas ASW-A varied more widely (67.8–

85.8 wt%), demonstrating that the filtration aid significantly influenced the HTC pathway. Ash content increased markedly in ASW-A (85.12–92.08 wt%) but only slightly in ASW-B (77.1–77.7 wt%), indicating that celite-based residues promoted more extensive decomposition of exposed organic matter during HTC.

In contrast, perlite-based residues restrained thermochemical degradation through stronger mineral–organic interactions. SEM observations support this mechanism, showing that organic material surrounding celite particles in ASW-A was relatively loosely associated, allowing greater exposure to hydrothermal reactions, whereas the organic fraction in ASW-B was more integrated with perlite particles, restricting decomposition and contributing to its relatively stable elemental composition during HTC. The resulting hydrochars remain unsuitable for conventional fuel applications because of their excessive ash contents. Mineral reduction strategies such as acid leaching, flotation, or selective deashing, together with integrated pretreatment–HTC systems, are therefore essential to improve energy applications. Future research should also examine mineral transformation mechanisms and liquid and gaseous product distributions to better assess ASW's overall resource-recovery potential.

ACKNOWLEDGMENT

The authors gratefully acknowledge financial support from BPPT under the Ministry of Higher Education, Republic of Indonesia, and LPDP under the Ministry of Finance, Republic of Indonesia. Additional funding was received from the Ministry of Higher Education, Malaysia, under Grant No. HICOE-2023-005. We conducted sample analyses using facilities at the National Research and Innovation Agency (BRIN), SBRC of IPB University, the Mechanical Engineering Laboratory of Universitas Mercu Buana, and ICRIM of Universiti Kebangsaan Malaysia (UKM). The authors also extend their sincere appreciation to the Indonesian Seaweed Processor Association (ASTRULI) for providing access for collecting agar solid waste samples.

REFERENCES

[1] M. Muryanto *et al.*, "Characterization of solid waste biomass of agar processing plants and scale-up production of bioethanol," *Biomass Convers. Biorefin.*, vol. 14, no. 18, pp. 22357–22366, 2024, doi: 10.1007/s13399-023-04464-7.

[2] F. S. Tadeo *et al.*, "Biochemical profiling of *Gracilaria edulis* agar waste for aquaculture applications," *Egypt. J. Aquat. Biol. Fish.*, vol. 29, no. 4, pp. 3139–3156, Jul. 2025, doi: 10.21608/EJABF.2025.449750.

[3] J. Basmal, I. Munifah, M. Rimmer, and N. Paul, "Identification and characterization of solid waste from *Gracilaria sp.* extraction," *IOP Conf. Ser. Earth Environ. Sci.*, vol. 404, Art. no. 012057, Jan. 2020, doi: 10.1088/1755-1315/404/1/012057.

[4] I. Munifah, J. Basmal, R. Kusumawati, and H. E. Irianto, "Cellulase derived from *Chryseobacterium indologenes* LA4K isolated from Indonesian agar-agar industry solid waste," *IOP Conf. Ser. Earth Environ. Sci.*, vol. 462, Art. no. 012007, Mar. 2020, doi: 10.1088/1755-1315/462/1/012007.

[5] A. Yulistian, E. N. Dewi, and L. Purnamayati, "Effect of agar industry waste-based liquid fertilizer on growth and nutrient uptake in red lettuce," *J. Soil Plant Environ.*, vol. 4, no. 1, pp. 31–46, 2025, doi: 10.56946/jspae.v4i1.649.

[6] G. Wangge, Y. V. Servianus, and T. Rande, "Utilization of plastic waste and rice husk ash in polyethylene-based composites for ceiling applications," *Int. J. Innov. Mech. Eng. Adv. Mater.*, vol. 7, no. 3, pp. 162–172, Jan. 2026, doi: 10.22441/ijimeam.v7i3.36658.

[7] M. Sidik, M. A. M. Sidik, A. M. Leman, D. Feriyanto, S. S. Abdulmalik, and S. Zakaria, "Green technology for sustainable agriculture: Bio-fertilizer production from municipal waste to preserve the environment," *Int. J. Innov. Mech. Eng. Adv. Mater.*, vol. 5, no. 3, pp. 118–124, Jan. 2024, doi: 10.22441/ijimeam.v5i3.23743.

[8] M. D. Bakri, E. Utomo, and D. Nawir, "Linear regression analysis on predicting the level of damage and changes in Amal Baru Beach, Tarakan City, Indonesia," *Sinergi*, vol. 27, no. 1, pp. 133–140, Jan. 2023, doi: 10.22441/sinergi.2023.1.015.

[9] A. Ariri, S. Alva, and S. A. Hasbullah, "Tire waste as a potential material for carbon electrode fabrication: A review," *Sinergi*, vol. 25, no. 1, pp. 1–10, Nov. 2020, doi: 10.22441/sinergi.2021.1.001.

[10] M. M. Naeem *et al.*, "Influence of externally added organic or inorganic acids on evolution of property of hydrochar from hydrothermal carbonization of potato peel," *Biomass Bioenergy*, vol. 204, Art. no. 108393, Jan. 2026, doi: 10.1016/j.biombioe.2025.108393.

[11] E. Kurniawan, R. Jariyaboon, A. Reungsang, T. Chucheep, and P. Kongjan, "Optimization of hydrothermal carbonization parameters of sugarcane residues for enhanced hydrochar fuel properties with ammonium adsorption assessment," *Chem. Eng. Sci.*, vol. 320, Art.

no. 122576, Jan. 2026, doi: 10.1016/j.ces.2025.122576.
[12] M. V. de Oliveira, A. F. Kanaan, F. A. P. Voll, and M. L. Corazza, "Hydrothermal carbonization of digestate from sewage sludge: Evaluating the impact of process parameters in hydrochar yield and characterization," *Fuel*, vol. 405, Art. no. 136672, Feb. 2026, doi: 10.1016/j.fuel.2025.136672.
[13] H. Zhang, G. Xue, H. Chen, X. Li, and S. Chen, "Revealing the heating value characteristics of sludge-based hydrochar in hydrothermal process: From perspective of hydrolysate," *Water Res*., vol. 198, Art. no. 117170, Jun. 2021, doi: 10.1016/j.watres.2021.117170.
[14] O. Farobie *et al*., "Valorization of *Ulva lactuca* via hydrothermal carbonization: Effects of temperature, time, and concentration on hydrochar," *J. Pengolah. Has. Perikan. Indones*., vol. 29, no. 2, pp. 161–177, Mar. 2026, doi: 10.17844/f3kztf96.
[15] O. Farobie *et al*., "Green algae to green fuels: Syngas and hydrochar production *from Ulva lactuca* via sub-critical water gasification," *Algal Res*., vol. 67, Art. no. 102834, Sep. 2022, doi: 10.1016/j.algal.2022.102834.
[16] Y. Yao, P. Xia, L. Zhao, C. Yang, R. Huang, and K. Wang, "Effects of temperature and duration on the combustion characteristics of hydrochar prepared from traditional Chinese medicine residues using hydrothermal carbonization process," *Int. J. Energy Res*., vol. 2024, Art. no. 3595643, 2024, doi: 10.1155/er/3595643.
[17] X. Su *et al*., "Potential application performance of hydrochar from kitchen waste: Effects of salt, oil, moisture, and pH," *Toxics*, vol. 11, no. 8, Art. no. 679, Aug. 2023, doi: 10.3390/toxics11080679.
[18] A. Škorjanc, D. Goričanec, and D. Urbancl, "Assessing energy potential and chemical composition of food waste thermodynamic conversion products: A literature review," *Energies*, vol. 17, no. 8, Art. no. 1897, Apr. 2024, doi: 10.3390/en17081897.
[19] D. Djaenudin, D. Permana, M. Ependi, and H. Putra, "Experimental studies on hydrothermal treatment of municipal solid waste for solid fuel production," *J. Ecol. Eng.,* vol. 22, no. 9, pp. 208–215, Oct. 2021, doi: 10.12911/22998993/141588.
[20] M. F. Rifandi, Djaenudin, H. E. Putra, and M. R. Sururi, "Optimization of traditional market solid waste conversion process into hydrochar using hydrothermal carbonization technology," *IOP Conf. Ser. Earth Environ. Sci*., vol. 1388, Art. no. 012033, Sep. 2024, doi: 10.1088/1755-1315/1388/1/012033.
[21] H. Durak, R. Z. Yarbay, and B. A. Türkmen, "Hydrothermal carbonization of biomass for hydrochar production: Mechanisms, process parameters, and sustainable valorization," *Processes*, vol. 14, no. 2, Art. no. 339, Jan. 2026, doi: 10.3390/pr14020339.
[22] Z. Li *et al*., "Optimized strategy for simultaneous recovering bioactive oligosaccharides and reusable perlite from agar industrial waste residues," *J. Clean. Prod*., vol. 378, Art. no. 134631, Dec. 2022, doi: 10.1016/j.jclepro.2022.134631.
[23] W. Fathonah, D. E. Intari, E. Mina, R. I. Kusuma, and E. S. Maryam, "Comparative analysis of increasing CBR value of soil with adding bamboo leaf ash," *Teknika J. Sains Teknol*., vol. 17, no. 2, pp. 277–284, Nov. 2021, doi: 10.36055/tjst.v17i2.13009.
[24] Y. Wahyono, H. Hadiyanto, W. Z. Pratiwi, and I. Dianratri, "'Biopellet' as one of future promising biomass-based renewable energy: A review," *E3S Web Conf*., vol. 317, Art. no. 04029, Nov. 2021, doi: 10.1051/e3sconf/202131704029.
[25] L. Wang, G. Skjevrak, and Ø. Skreiberg, "Investigation on ash slag from combustion of medium-density fiberboard production residues," *DEStech Trans. Environ. Energy Earth Sci.*, no. PEEMS, Apr. 2020, doi: 10.12783/dteees/peems2019/33931.
[26] D. A. Roberts, N. A. Paul, S. A. Dworjanyn, Y. Hu, M. I. Bird, and R. de Nys, "*Gracilaria* waste biomass as a bioresource for selenium biosorption," *J. Appl. Phycol.*, vol. 27, pp. 611–620, May 2015, doi: 10.1007/s10811-014-0346-y.
[27] T. J. Hasiweder, H. M. Dinh, D. K. Pandey, A. Sorvanov, and J. R. Khusnutdinova, "Mechanoactivated celite as a catalyst for C–H bond perfluoroalkylation and other radical reactions," *Angew. Chem. Int. Ed.*, vol. 64, Art. no. e202504137, Aug. 2025, doi: 10.1002/anie.202504137.
[28] R. A. Zamara, L. A. Yudhana, C. A. Curie, and M. Gozan, "Stability and esterification activity of *Candida rugosa* lipase immobilized on celite with acetone solvent," *IOP Conf. Ser. Earth Environ. Sci*., vol. 1187, Art. no. 012038, May 2023, doi: 10.1088/1755-1315/1187/1/012038.
[29] D. A. Darmawan, A. Wahyudi, H. E. Mamby, and I. Suherman, "Characterization of perlite and expanded perlite from West Sumatera, Indonesia," *IOP Conf. Ser. Earth Environ. Sci*., vol. 882, Art. no. 012010, Nov. 2021, doi: 10.1088/1755-1315/882/1/012010.

[30] O. Farobie *et al*., "Simultaneous production of nutritional compounds and hydrochar from *Chlorella pyrenoidosa* via hydrothermal process," *Bioresour. Technol. Rep*., vol. 20, Art. no. 101245, Dec. 2022, doi: 10.1016/j.biteb.2022.101245.

[31] A. Demirbas and M. F. Demirbas, "Energy from Algae," in *Algae Energy*, ser. Green Energy and Technology. London, U.K.: Springer, 2010, ch. 5, pp. 97-138, doi: 10.1007/978-1-84996-050-2_6.

[32] P. Liu *et al*., "Effect of evolution of carbon structure during torrefaction in woody biomass on thermal degradation," *Int. J. Environ. Res. Public Health*, vol. 19, no. 24, Art. no. 16831, Dec. 2022, doi: 10.3390/ijerph192416831.

[33] A. Shrestha, B. Acharya, and A. A. Farooque, "Study of hydrochar and process water from hydrothermal carbonization of sea lettuce," *Renew. Energy*, vol. 163, pp. 589–598, Jan. 2021, doi: 10.1016/J.RENENE.2020.08.133.

[34] A. F. Sudarma *et al.*, "Demineralization of silica-rich agar processing residues via hydrofluoric acid leaching for organic fraction enrichment," *Int. J. Innov. Mech. Eng. Adv. Mater.*, vol. 8, no. 2, 2026, doi: 10.22441/ijimeam.v8i2.38546.

[35] S. B. Prasetyati, H. N. Lioe, N. D. Yuliana, A. B. Sitanggang, and A. Permadi, "Proximate composition and infra-red spectra profiles of *Gracilaria sp.* from five harvest locations," *J. Pengolah. Has. Perikan. Indones.*, vol. 29, no. 1, pp. 15–28, Feb. 2026, doi: 10.17844/85QBHC79.

[36] Z. Sui, J. Wu, J. Wang, Y. Cao, Q. Wang, and W. Chen, "Effect of hydrothermal carbonization temperature on fuel properties and combustion behavior of high-ash corn and rice straw hydrochar," *Therm. Sci.*, vol. 27, no. 4A, pp. 2651–2664, 2023, doi: 10.2298/TSCI220813186S.

[37] O. Sadish, S. P. Sebastian, K. S. P. Banu, and R. Mahendran, "Hydrochar as an energy alternative to coal: Effect of temperature on hydrothermal carbonization of paper board mill sludge," *Int. J. Curr. Microbiol. Appl. Sci.*, vol. 8, no. 6, pp. 1668–1675, Jun. 2019, doi: 10.20546/ijcmas.2019.806.199.

[38] Y. Li *et al*., "Rice husk hydrochars from metal chloride-assisted hydrothermal carbonization as biosorbents of organics from aqueous solution," *Bioresour. Bioprocess*., vol. 8, Art. no. 99, Dec. 2021, doi: 10.1186/s40643-021-00451-w.

[39] H. Liu *et al.*, "Hydrothermal treatment of high ash microalgae: Focusing on the physicochemical and combustion properties of hydrochars," *Energy Fuels*, vol. 34, no. 2, pp. 1929–1939, Feb. 2020, doi: 10.1021/acs.energyfuels.9b04093.

[40] Y. Li, F. Chang, B. Huang, Y. Song, H. Zhao, and K. Wang, "Activated carbon preparation from pyrolysis char of sewage sludge and its adsorption performance for organic compounds in sewage," *Fuel*, vol. 266, Art. no. 117053, Apr. 2020, doi: 10.1016/j.fuel.2020.117053.

[41] İ. Kırbaş, "Effect of perlite on the thermal conductivity, thermal degradation and mechanical properties of epoxy materials," *High Perform. Polym.*, vol. 34, no. 8, pp. 880–888, Oct. 2022, doi: 10.1177/09540083221092147.

[42] N. Syaftika *et al.*, "Hydrogen and hydrochar production from *Ulva lactuca* via subcritical and supercritical water gasification with formic acid addition," *Evergreen*, vol. 13, no. 1, pp. 188–199, Mar. 2026, doi: 10.5109/7407644.

[43] A. Amrullah, O. Farobie, and W. Fatriasari, "Catalytic upgrading of bio-oil from *Ulva lactuca* using Amberlyst-15 catalyst: Experimental and kinetic model," *Int. J. Eng.*, vol. 36, no. 10, pp. 1677–1685, 2023, doi: 10.5829/IJE.2023.36.09C.12.

[44] K. Mehrez *et al.*, "Hydrothermal treatment of contaminated sorghum: Hydrochar properties and characterization/phytotoxicity evaluation of the liquid phase," *J. Environ. Chem. Eng.*, vol. 13, no. 5, Art. no. 117710, Oct. 2025, doi: 10.1016/j.jece.2025.117710.

[45] J. Xiong *et al.*, "Study on the hydrothermal carbonization of swine manure: The effect of process parameters on the yield/properties of hydrochar and process water," *J. Anal. Appl. Pyrolysis*, vol. 144, Art. no. 104692, Nov. 2019, doi: 10.1016/j.jaap.2019.104692.

[46] V. S. Ekanthalu, S. Narra, T. Ender, E. Antwi, and M. Nelles, "Influence of post- and pre-acid treatment during hydrothermal carbonization of sewage sludge on P-transformation and the characteristics of hydrochar," *Processes*, vol. 10, no. 1, Art. no. 151, Jan. 2022, doi: 10.3390/pr10010151.

[47] T.-S. Shin *et al*., "Analysis of hydrothermal solid fuel characteristics using waste wood and verification of scalability through a pilot plant," *Processes*, vol. 10, no. 11, Art. no. 2315, Nov. 2022, doi: 10.3390/pr10112315.